THE JOURNAL OF BIOLOGICAL CHEMISTRY VOL. 292, NO. 14, pp. 5981–5991, April 7, 2017

The hypoxia-inducible factors HIF1α and HIF2α are dispensable for embryonic muscle development but essential for postnatal muscle regeneration

Received for publication, August 30, 2016, and in revised form, February 22, 2017 Published, JBC Papers in Press, February 23, 2017, DOI 10.1074/jbc.M116.756312

Xin Yang[‡1], **Shiqi Yang**[‡1], **Chao Wang**[‡], **and Shihuan Kuang**[‡§2]

From the [‡]*Department of Animal Science, Purdue University and* [§]*Purdue University Center for Cancer Research, West Lafayette, Indiana 47907*

Edited by Velia M. Fowler

Muscle satellite cells are myogenic stem cells whose quiescence, activation, self-renewal, and differentiation are influenced by oxygen supply, an environmental regulator of stem cell activity. Accordingly, stem cell-specific oxygen signaling pathways precisely control the balance between muscle growth and regeneration in response to oxygen fluctuations, and hypoxia-inducible factors (HIFs) are central mediators of these cellular responses. However, the *in vivo* roles of HIFs in quiescent satellite cells and activated satellite cells (myoblasts) are poorly understood. Using transgenic mouse models for cell-specific HIF expression, we show here that HIF1α and HIF2α are preferentially expressed in pre- and post-differentiation myoblasts, respectively. Interestingly, double knockouts of HIF1α and HIF2α (HIF1α/2α dKO) generated with the MyoD^{Cre} system in embryonic myoblasts resulted in apparently normal muscle development and growth. However, HIF1α/2α dKO produced with the tamoxifen-inducible, satellite cell-specific Pax7^{CreER} system in postnatal satellite cells delayed injury-induced muscle repair due to a reduced number of myoblasts during regeneration. Analysis of satellite cell dynamics on myofibers confirmed that HIF1α/2α dKO myoblasts exhibit reduced self-renewal but more pronounced differentiation under hypoxic conditions. Mechanistically, the HIF1α/2α dKO blunted hypoxia-induced activation of Notch signaling, a key determinant of satellite cell self-renewal. We conclude that HIF1α and HIF2α are dispensable for muscle stem cell function under normoxia but are required for maintaining satellite cell self-renewal in hypoxic environments. Our insights into a critical mechanism in satellite cell homeostasis during muscle regeneration could help inform research efforts to treat muscle diseases or improve muscle function.

Satellite cells are the stem cells of skeletal muscle and the cellular source of muscle development, growth, and regeneration (1–4). Satellite cells can not only undergo myogenic differentiation to supply myonuclei to growing and regenerating muscles but also self-renew to maintain the stem cell population (5–7). The balance between self-renewal and differentiation must be precisely controlled to maintain sustainable muscle growth and regeneration (8–10). Defective myogenic differentiation during embryonic development may lead to postnatal muscle atrophy, whereas insufficient self-renewal largely reduces satellite cell population and leads to failure of muscle regeneration in adults (11, 12). Cell fate determination is controlled by both cell intrinsic and extrinsic regulatory mechanisms including extracellular microenvironmental cues (13, 14).

Oxygen is absolutely critical for life and is one of the most important microenvironmental cues that regulates cellular energy metabolism and survival. During embryonic development, the fetus grows in a relatively less oxygenated or hypoxic environment (15, 16). In adults, satellite cells also reside in a hypoxic microenvironment (16). Hypoxia-inducible factors (HIFs)[3] are the primary transcription factors mediating the cellular response to low O_2 tensions or hypoxia (17). HIFs consist of O_2-sensitive α-subunits and O_2-insensitive β-subunits. Under normoxia, HIFα subunits are hydroxylated at the proline residue and subjected to ubiquitination and proteolytic degradation. Hypoxia blocks this hydroxylation and stabilizes HIFα subunits, which then form heterodimers with HIFβ units to generate the transcriptional active complex. The dimeric HIFα/HIFβ specifically binds to conserved hypoxia-responsive element to regulate transcription of target genes (17).

There are three known isoforms of HIFα subunits, namely HIF1α, HIF2α, and HIF3α (16–18). Whereas the functions of HIF1α and HIF2α are relatively well known, very little is known about the function of HIF3α due to its late discovery and low expression levels (18–22). Overall, HIFs play distinct and overlapping functions in various tissue and cell types.

In the adult skeletal muscle, exercise induces HIF1α expression, and myofiber-specific disruption of HIF1α results in a decrease in exercise endurance, suppression of oxidative metabolism, and attenuation of glucose transporter 4 (GLUT4)-

This work was supported by a research grant (#294644) from the Muscular Dystrophy Association (to S. K.). The authors declare that they have no conflicts of interest with the contents of this article.
This article contains supplemental Table 1 and Figs. 1 and 2.
[1] Both authors contributed equally to this work.
[2] To whom correspondence should be addressed. E-mail: skuang@purdue.edu.

[3] The abbreviations used are: HIF, hypoxia-inducible factor; EDL, extensor digitorum longus; CTX, cardiotoxin; DPI, days post injury; TA, tibialis anterior; 4-OH-TMX, 4-hydroxyl tamoxifen; Ad, adenovirus; NICD, Notch1 intercellular domain; dKO, double knockout; qPCR, quantitative real-time PCR.

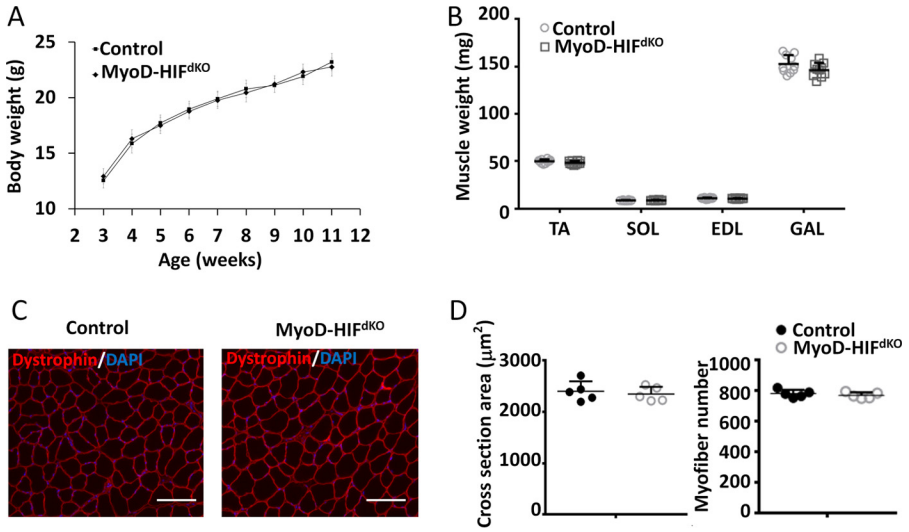

Figure 1. MyoD^{Cre}-mediated double knock-out of HIF1α and HIF2α (MyoD-HIF^{dKO}) did not affect muscle development and growth. *A*, growth curve of MyoD-HIF^{dKO} and control mice, $n = 10$ pairs. *B*, weights of TA, soleus (*SOL*), EDL, and gastrocnemius (*GAS*) muscles of MyoD-HIF^{dKO} and control mice. $n = 10$ pairs. *C*, representative images of EDL muscle cross-section from 2 months old MyoD-HIF^{dKO} and control mice. *Scale bar*: 50 μm. *D*, quantification of myofiber size and myofiber number from EDL muscles for MyoD-HIF^{dKO} and control mice ($n = 5$ pairs). *Error bars* represent S.D.

mediated glucose uptake (23, 24). Global deletion of HIF2α in mice results in ectopic fat deposition in the skeletal muscle (25). Interestingly, HIF1α and HIF2α play distinct roles in fast and slow myofibers. HIF1α plays a role in fast myofiber formation (26, 27). In contrast, HIF2α acts as a positive regulator of slow fiber type through acting downstream of peroxisome proliferator-activated receptor-γ coactivator 1α (PGC-1α) (25). HIF3α mRNA level is elevated in skeletal muscle after acute exposure to hypoxia or after intermittent hypoxia training, and HIF3α RNAi-treated rats had improved exercise endurance (28). These data suggest that HIFs play key roles in maintaining metabolic and contractile functions of myofibers in adult muscles.

Emerging studies also point to a role of HIF1α in muscle progenitors (myoblasts) *in vitro*. HIF1α protein is stabilized in cultured myoblasts under hypoxia (20), but the function of HIF1α in myoblasts has been controversial. For example, Gustafsson *et al.* (31) and Majmundar *et al.* (30) reported that hypoxia-induced HIF1α accumulation inhibited myoblast differentiation. By contrast, Ono *et al.* (29) reported that HIF1α knock down inhibited myoblast differentiation under normoxia conditions (30, 31). These results underscore the context-dependent function of HIF1α and further suggest that HIF1α may also function as signaling regulators in addition to their canonical role as a transcription factor (23, 30, 32). Recently, it was reported that HIF1α inhibited ischemia-induced muscle regeneration through inhibiting Wnt signaling (30).

Together, despite the wealthy knowledge of HIF1α and HIF2α in post-differentiation myofibers, the function of HIF1α and HIF2α in muscle stem cells *in vivo* is poorly understood. In this study we used MyoD^{Cre} knockin mice to drive co-deletion of HIF1α and HIF2α, in order to determine the function of HIF1α/HIF2α in embryonic myoblasts. We further used tamoxifen-inducible Pax7^{CreER} mice to drive HIF1α/HIF2α deletion in postnatal satellite cells. We provided the first evidence that HIF1α and HIF2α are dispensable for normal development of skeletal muscles but necessary for proper regeneration of adult muscles after acute injury. Therefore, HIFs play context-dependent roles in embryonic myoblasts and postnatal satellite cells.

Results

MyoD^{Cre}-mediated double knock-out of HIF1α and HIF2α did not affect muscle development

Previous studies have shown that HIF1α are indispensable for embryonic development, and global loss of HIF1α leads to lethality (16, 33, 34). HIF2α-deficient mice develop severe vascular defects and show developmental arrest between E9.5 and E12.5 depending on the genetic background (33, 35). Hence, the specific function of HIFs in muscle development remains unclear. As Pax3^{Cre}-mediated deletion of HIF1α results in apparently normal skeletal muscles (30), we sought to examine whether HIF1α and HIF2α play redundant roles in muscle development. To achieve this we developed the HIF1α and HIF2α double knock-out mouse model using the muscle-specific MyoD^{Cre} as a driver (MyoD-HIF^{dKO}). Because MyoD is specifically and ubiquitously activated in early embryonic myoblasts, this model should result in deletion of HIF1α and HIF2α in all muscle progenitors and mature myofibers (7, 10).

Surprisingly, the MyoD-HIF^{dKO} mice were born at a normal Mendelian ratio and did not exhibit any morphological abnormality. Specifically, the initial body weight and postnatal growth of MyoD-HIF^{dKO} mice were completely normal (Fig. 1*A*). Furthermore, the weight and size of various muscles were identical between control and MyoD-HIF^{dKO} mice (Fig. 1*B*). Muscle morphology was also indistinguishable between the two groups (Fig. 1*C*). Finally, we measured myofiber number and size of extensor digitorum longus (EDL) muscles and did not find any differences between control and MyoD-HIF^{dKO} mice (Fig. 1*D*). These results suggest that HIF1α and HIF2α are dispensable for skeletal muscle development and postnatal growth under normal oxygen conditions.

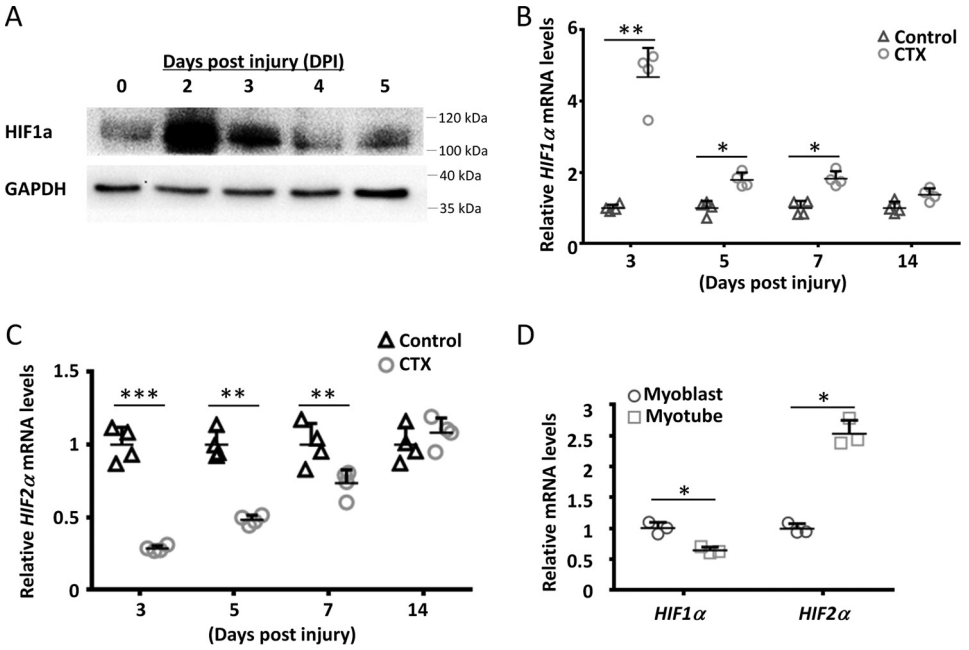

Figure 2. Muscle injury up-regulated expression of HIF1α and HIF2α. *A–C*, HIF1α protein (*A*), *HIF1α* mRNA (*B*, $n = 4$ pairs), and *HIF2α* mRNA (*C*, $n = 4$ pairs) levels at various time points after cardiotoxin-induced muscle injured. *D*, *HIF1α* and *HIF2α* mRNA levels in proliferating myoblasts and post-differentiation myotubes. $n = 3$ cultures. Relative levels of mRNA were determined by qPCR. *Error bars* represent S.D. *, $p < 0.05$; **, $p < 0.01$; ***, $p < 0.005$ (Student's *t* test, two-tailed).

Knock-out of HIF1α and HIF2α in satellite cells impedes muscle regeneration

The normal development and growth of skeletal muscles in the MyoD-HIF^{dKO} mice suggest that coordinated angiogenesis and myogenesis may have ensured adequate oxygen supply and rendered HIF1α and HIF2α dispensable for embryonic myogenesis. By contrast, ischemic low oxygen levels (hypoxia) typically occur after muscle injury and during muscle regeneration (36). Indeed, examination of HIF1α and HIF2α expression indicates that HIF1α protein and mRNA levels rise after cardiotoxin (CTX)-induced muscle injury, peaking at 2–3 days post injury (DPI) when active myoblast proliferation occurs (Fig. 2, *A* and *B*). However, *HIF2α* levels decrease dramatically upon injury-induced myofiber degeneration and gradually return to the normal level at the completion of muscle regeneration (Fig. 2*C*). The *in vivo* dynamics of *HIF1α* and *HIF2α* during muscle regeneration suggest that *HIF1α* is mainly expressed in myoblasts, but *HIF2α* is mainly expressed in myofibers. Consistent with this notion, the mRNA level of *HIF1α* is much higher than that of *HIF2α* in proliferating myoblasts (Fig. 2*D*). In contrast, the mRNA level of *HIF2α* is much higher than that of *HIF1α* in post-differentiation myotubes (Fig. 2*D*). These results suggest that regenerative muscles are challenged by hypoxia, and HIF1α and HIF2α may play stage-specific functions in myoblasts and myofibers, respectively.

To identify the role of HIF1α and HIF2α in satellite cell-mediated muscle regeneration, we used satellite cell-specific Pax7^{CreER} to drive double knock-out of HIF1α and HIF2α (Pax7^{CreER}-HIF^{dKO}) (8–10). In this model, HIF1α and HIF2α should be specifically knocked out in satellite cells after tamoxifen induction (i.p. injection). This model also circumvents the cofounding effects of HIF1α/HIF2α KO in myofibers in the MyoD-HIF^{dKO} mice. The control group includes HIF1α$^{f/f}$ HIF2α$^{f/f}$ mice similarly injected with tamoxifen. To confirm the efficiency of tamoxifen-induced knock-out, we measured the *HIF1α* and *HIF2α* mRNA levels in satellite cells isolated from tamoxifen-induced mice (supplemental Fig. S1). This analysis showed that HIF1α and HIF2α were efficiently knocked out in myoblasts.

After tamoxifen-induced deletion of HIF1α and HIF2α in satellite cells, CTX was injected into tibialis anterior (TA) muscle to induce ischemic muscle injury in both control and Pax7^{CreER}-HIF^{dKO} mice. Samples were collected 7 and 21 days post CTX injection (Fig. 3*A*; see Fig. 5*A*). Compared with those of control mice, the CTX-injected TA muscles of Pax7^{CreER}-HIF^{dKO} mice exhibited decreased sizes and significantly lower weights at 7 DPI (Fig. 3, *B* and *C*). In addition, TA muscles of Pax7^{CreER}-HIF^{dKO} mice were poorly regenerated, manifested by fewer newly regenerated, central nucleated myofibers (Fig. 3*D*). We also measured the regenerated and non-regenerated areas from cross sections of control mice and Pax7^{CreER}-HIF^{dKO} mice. Pax7^{CreER}-HIF^{dKO} mice exhibited a smaller regenerative area as well as a larger non-regenerative region than the littermate control mice (Fig. 3*E*). However, no morphological differences were observed in regenerated muscles between the control and Pax7^{CreER}-HIF dKO groups at 21 DPI (see Fig. 5, *B* and *C*). Thus, satellite cell-specific HIF1α and HIF2α deficiency delayed muscle regeneration after acute injuries.

HIF1α and HIF2α deficiency decreases satellite cell number during muscle regeneration

As satellite cells are the main contributors of muscle regeneration (37), we next investigated if the delayed muscle regeneration is associated with reduced satellite cell number or function. To assess the satellite cell numbers, we used Pax7 and

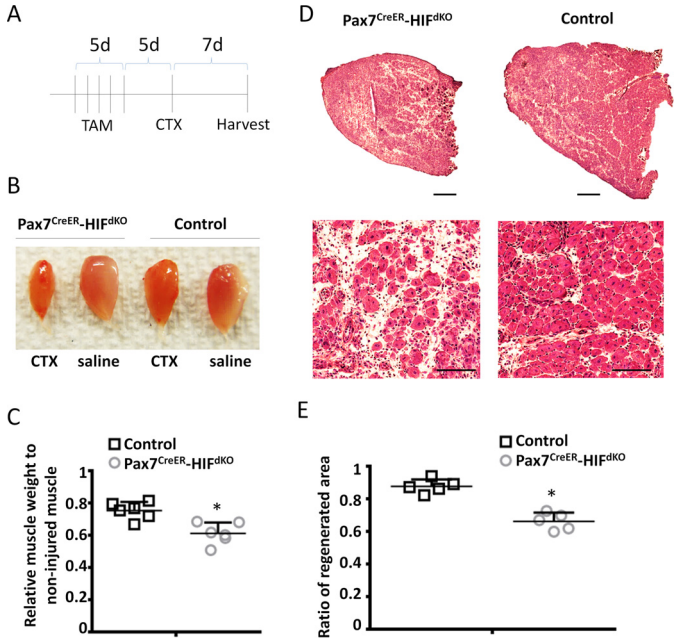

Figure 3. Impaired muscle regeneration in Pax7^{CreER}-HIF^{dKO} mice at 7 days post injury. *A*, experimental design. Tamoxifen (*TAM*) was i.p.-injected daily into Pax7^{CreER}HIF1$\alpha^{f/f}$HIF2$\alpha^{f/f}$ and HIF1$\alpha^{f/f}$HIF2$\alpha^{f/f}$ mice for 5 days to activate CreER and induce deletion of HIF1α and HIF2α. Muscle injury was induced by injection of CTX. Saline injection into the contralateral TA muscles was performed as non-injury controls. Samples were collected 7 days post injury. *B*, representative photos of TA muscles 7 days after injury. *C*, relative weight of TA muscles after regeneration, as shown in *B*. $n = 6$ pairs. *D*, representative images of whole muscle sections (*scale bar*: 500 μm) and magnified regenerated regions (*scale bar*: 50 μm). *E*, quantification of regenerated and non-regenerated areas based on cross sectional staining, as depicted in *D*. $n = 5$ pairs. *Error bars* represent S.D. *, $p < 0.05$ (Student's *t* test, two-tailed).

CD34 to label satellite cells (38, 39). Pax7-positive cells were measured in both non-injured (saline-treated) and injured (CTX-treated) TA muscles of Pax7^{CreER}-HIF^{dKO} and control mice (Fig. 4*A*). In the non-injured muscles, the abundances of Pax7$^+$ cells were identical between control and Pax7^{CreER}-HIF^{dKO} muscle (Fig. 4*B*), suggesting that co-deletion of HIF1α and HIF2α does not affect satellite cells in non-injured resting muscles. In the injured muscles, however, there were significantly fewer numbers of Pax7$^+$ cells per TA cross-sectional areas in Pax7^{CreER}-HIF^{dKO} mice compared with control mice at 7 DPI (Fig. 4*B*). To confirm this observation, we also counted Pax7$^+$/CD34$^+$ satellite cells in fresh-isolated EDL myofibers (Fig. 4*C*). Consistent with the TA muscle cross-section results, the numbers of satellite cells per myofiber were identical between control and Pax7^{CreER}-HIF^{dKO} mice in non-injured muscles, but the Pax7^{CreER}-HIF^{dKO} mice had significantly fewer satellite cells after CTX injury at both 7 and 21 DPI (Fig. 4*D*; see Fig. 5*D*). These results indicate that although co-deletion of HIF1α and HIF2α does not reduce satellite cells in non-injured muscles, it impairs injury-induced satellite cell proliferation or self-renewal, leading to a reduced number of satellite cells during and after muscle regeneration.

HIF1α and HIF2α deficiency inhibits self-renewal but promotes differentiation of satellite cells

To understand if the reduced number of satellite cells in the Pax7^{CreER}-HIF^{dKO} mice during and after regeneration is due to deficiencies in proliferation or self-renewal (4, 40), we performed cell culture assays. To acutely induce HIF1α and HIF2α deletion in cultured myoblasts, we isolated myoblasts from Pax7^{CreER}-HIF1$\alpha^{f/f}$HIF2$\alpha^{f/f}$ and HIF1$\alpha^{f/f}$HIF2$\alpha^{f/f}$ mice and then treated the primary myoblasts with 4-hydroxyl tamoxifen (4-OH-TMX, 40 nM) for 2 days. This treatment led to a >95% reduction in the mRNA levels of *HIF1α* and *HIF2α* (supplemental Fig. S1*C*).

After 72 h of culture, we labeled cells with Pax7 and MyoD (Fig. 6*A*) and classified the cell status into self-renewal (Pax7$^+$/MyoD$^-$), proliferating (Pax7$^+$/MyoD$^+$), and differentiating (Pax7$^-$/MyoD$^+$) subpopulations (8–10). Under normoxia conditions (21% O_2), no differences in cell status distribution were observed between the control and HIF1α/HIF2α dKO groups (Fig. 6*B*). Under hypoxia (1% O_2) conditions, however, HIF1α/HIF2α dKO myoblasts exhibited significantly reduced self-renewal but increased differentiation without affecting proliferation (Fig. 6*B*). Consistent with our previous results (41), a higher rate of self-renewal was found in the hypoxia group (22%) compared with the normoxia group (11%) in control myoblasts. However, the hypoxia-enhanced self-renewal was largely diminished by HIF1α and HIF2α dKO (Fig. 6*B*), indicating that hypoxia promotes self-renewal through HIF1α and HIF2α.

Muscle satellite cells natively reside in a microenvironment surrounded by the sarcolemma and basal lamina (42). To mimic the impact of hypoxia on satellite cell self-renewal in a physiological microenvironment, we isolated EDL myofibers from Pax7^{CreER}-HIF^{dKO} and HIF1$\alpha^{f/f}$HIF2$\alpha^{f/f}$ mice. After culturing under either hypoxia or normoxia conditions for 72 h, satellite cells formed clusters of myoblasts, which were stained with Pax7 and MyoD to determine cell states (Fig. 6*C*). Consistent with our primary myoblast culture results, both control and HIF1α/HIF2α dKO satellite cells formed identical proportions of self-renewal (Pax7$^+$/MyoD$^+$), proliferating (Pax7$^+$/MyoD$^-$), and differentiating (Pax7$^-$/MyoD$^+$) cells under normoxia conditions (Fig. 6*D*). Under hypoxia conditions, however, HIF1α/HIF2α dKO reduced the proportion of self-renewal satellite cells and increased the proportion of differentiating cells without affecting the proportion of proliferating cells (Fig. 6*D*). Together, these results demonstrate that HIF1α/HIF2α dKO reduces self-renewal of satellite cells under hypoxia conditions.

HIF1α and HIF2α promote satellite cell self-renewal through notch signaling

Previous studies have shown that hypoxia activates Notch signaling, which subsequently promotes self-renewal and inhibits differentiation of myoblasts (31, 41). We, hence, hypothesized that HIF1α and HIF2α may promote satellite cell self-renewal through enhancing Notch signaling. To test this hypothesis, we induced deletion of HIF1α and HIF2α by adenovirus (Ad)-Cre/GFP transduction into HIF1$\alpha^{f/f}$HIF2$\alpha^{f/f}$ myoblasts. Ad-GFP was used in parallel as a control (supplemental Fig. S2*A*). At 24 h after adenovirus infection, the relative mRNA levels of *HIF1α* and *HIF2α* were dramatically reduced by the Ad-Cre infection (supplemental Fig. S2*B*). Ad-Cre also dramatically decreased the levels of HIF1α protein after stabi-

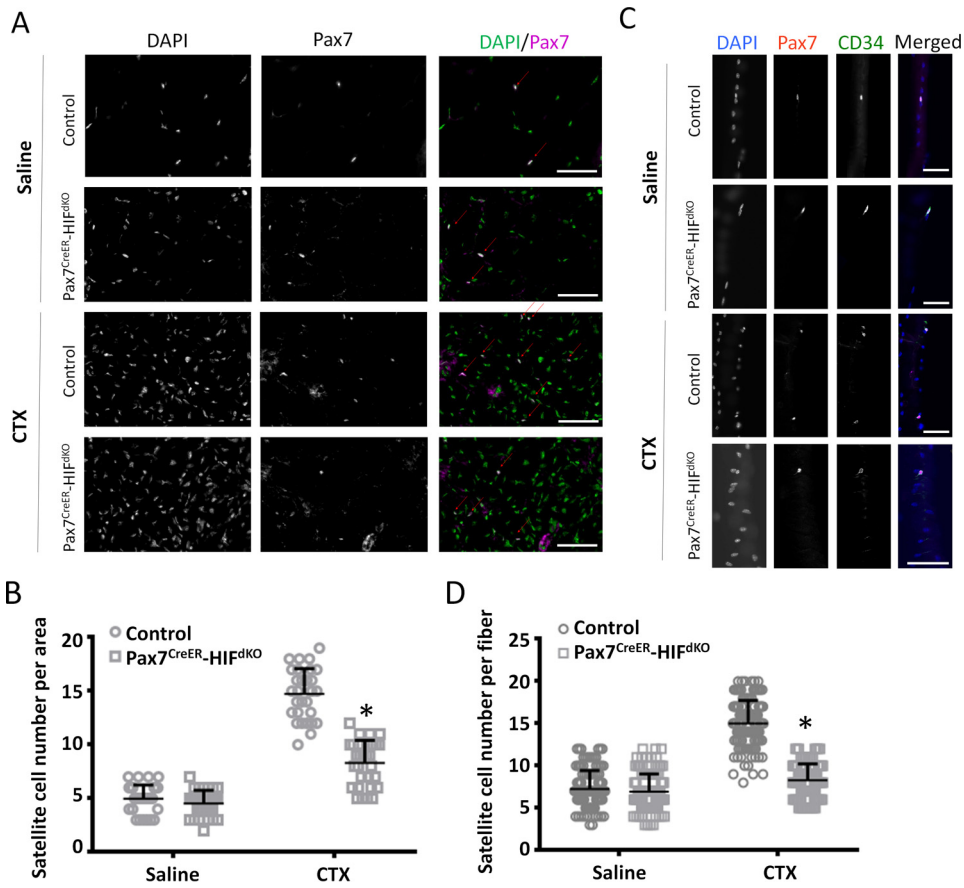

Figure 4. Reduced satellite cell number in skeletal muscles of Pax7^{Cre}-HIF^{dKO} mice after injury. *A*, representative images of Pax7 (indicated by the *arrows*) immunofluorescence in TA muscle sections of Pax7^{Cre}-HIF^{dKO} and control mice at 7 days after CTX or saline injection. Nuclei were counterstained with DAPI. *Scale bar*: 50 μm. *B*, quantification of Pax7^{+} satellite cells from TA muscle cross-sections as shown in *A*. Samples are collected from six pairs of animals (six control and six dKO mice). For each sample five random photos were analyzed for quantification of satellite cells. Data from individual photo are shown. *C*, representative images of Pax7 and CD34 immunofluorescence on freshly isolated EDL myofibers. *Scale bar*: 40 μm. *D*, quantification of Pax7^{+} and CD34^{+} cells in freshly isolated EDL myofibers. Samples are collected from 5 pairs of mice; 25 fibers from each mouse were used for quantifying satellite cells. Data from individual fibers are shown. *Error bars* represent S.D. *, $p < 0.05$ (Student's *t* test, two-tailed).

lizing with $CoCl_2$ (Fig. 7, *A* and *B*). These results confirm the high efficiency of Ad-Cre-mediated KO of *HIF1α* and *HIF2α*.

We next evaluated the extent of Notch activation based on the level of Notch1 intercellular domain (NICD), which is proteolytically cleaved after Notch activation (43, 44). Under normoxia conditions, NICD levels were similar between Ad-GFP and Ad-Cre-treated groups (Fig. 7*A*), suggesting that HIF1α and HIF2α dKO do not affect Notch activation under normoxia. However, after 6 h of $CoCl_2$ treatment (to stabilize HIFs and mimic hypoxia), NICD levels in the Ad-Cre-treated group were significantly lower than that in the Ad-GFP group (Fig. 7*B*). These results suggest that deletion of HIFs blunts hypoxia-induced activation of Notch in myoblasts. To further confirm this notion, we examined the expression of Notch target genes. In the Ad-GFP-treated control myoblasts, *Hes2* and *Hey2* were significantly increased, whereas *Hes6* was dramatically decreased by $CoCl_2$ treatment, indicating that hypoxia activates Notch signaling (Fig. 7*C*). By contrast, $CoCl_2$ treatment had no effects on the expression of Notch target genes in Ad-Cre-treated HIF1α/HIF2α dKO myoblasts (Fig. 7*D*). Furthermore, whereas $CoCl_2$ treatment significantly increased the level of *Pax7* in control myoblasts, it had no effect on *Pax7* expression in HIF1α/HIF2α dKO myoblasts (Fig. 7*E*).

To further define Notch signaling as a downstream target of HIF1α/HIF2α, we performed a luciferase reporter assay. Murine C2C12 myoblasts were transfected with the Renilla luciferase reporter (TP-1) containing the Rpbj binding domain that mediates the transcriptional activity of NICD. The transfected cells were cultured under normoxia and hypoxia in the absence or presence of FM19G11, a pharmacological inhibitor of HIF1α/HIF2α. Hypoxia up-regulated the TP-1 luciferase activity in the absence of FM19G11 (Fig. 7*F*). However, when HIF1α/HIF2α activity was suppressed by FM19G11, hypoxia could no longer activate the TP-1 luciferase activity (Fig. 7*F*). These results together demonstrate that HIF1α and HIF2α expression or activity is required for hypoxia-induced activation of Notch signaling and up-regulation of Pax7, the key transcriptional determinant of muscle stem cell fate.

We also tested if activation of Notch signaling can rescue the self-renewal defects of the HIF1α/HIF2α dKO myoblasts. To activate Notch signaling in myoblasts, we co-cultured myoblasts with OP9 cells that overexpress Dll1 (45, 46), a Notch ligand. After co-cultured for 72 h under hypoxia, we examined the cell status of myoblasts based on Pax7 and MyoD (Fig. 8*A*). Consistent with our hypothesis, HIF1α/HIF2α dKO myoblasts had self-renewal and differentiation ratios identical to the con-

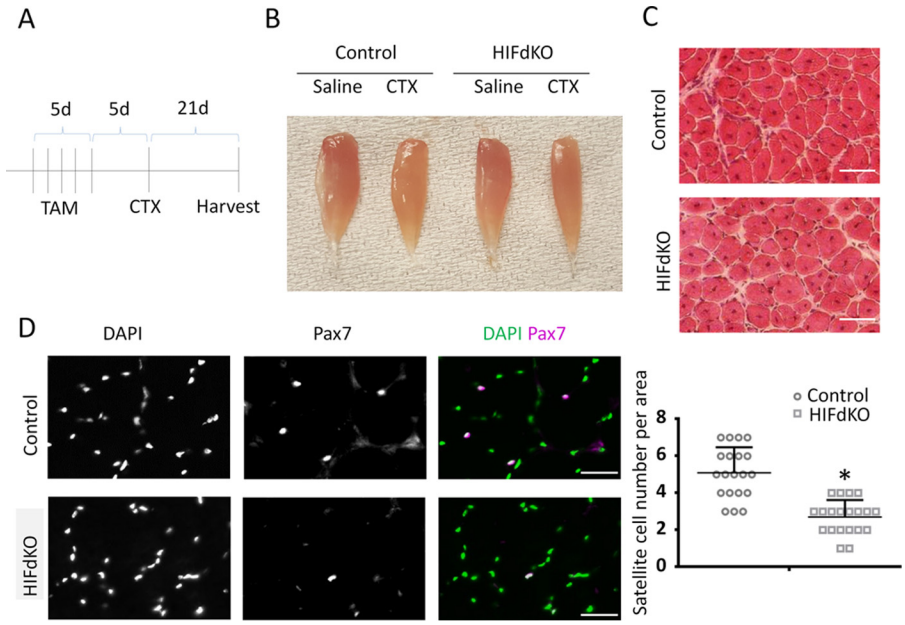

Figure 5. Reduced satellite cell number in skeletal muscles of Pax7^{Cre}-HIF^{dKO} mice 21 days after CTX-induced muscle injury. *A*, experimental design. Tamoxifen was i.p.-injected daily into Pax7^{CreER}HIF1$\alpha^{f/f}$HIF2$\alpha^{f/f}$ and HIF1$\alpha^{f/f}$HIF2$\alpha^{f/f}$ mice for 5 days to activate CreER and induce deletion of HIF1α and HIF2α. Muscle injury was induced by injection of CTX. Saline injection was used as non-injury control. Samples were collected 21 days after injury. *B*, representative photos of TA muscles 21 days after regeneration. *C*, representative H&E staining micrographs of TA muscle sections. *Scale bar*: 50 μm. *D*, representative images of Pax7 immunofluorescent labeling of satellite cells. Nuclei were counterstained with DAPI. *Scale bar*: 50 μm. Numbers of satellite cells per area in TA muscle sections 21 days after regeneration were shown in the *bar graphs*. Samples were collected from four pairs of control and HIF^{dKO} mice. For each sample, five random areas were analyzed for quantification of satellite cells. Data from each area are shown. *Error bars* represent S.D. *, $p < 0.05$ (Student's *t* test, two-tailed).

trol myoblasts (Fig. 8*B*). These results indicate that activation of Notch signaling is sufficient to rescue the self-renewal defect of HIF1α/HIF2α dKO myoblasts, confirming that HIF1α/HIF2α promote self-renewal of satellite cells through activating Notch signaling.

Discussion

Given the important role of HIFs in mediating hypoxia signaling, it is plausible to assume that their absence should affect muscle progenitor cell function during development. However, previous studies have shown that Pax3-driven knock-out of HIF1α in embryonic myoblasts does not muscle development (30), raising the possibility that HIF2α may have compensated the HIF1α loss-of-function. However, our results demonstrate that myoblast-specific HIF1α/HIF2α dKO mice exhibited normal muscle development and normal myofiber size and number in the adult. These results suggest that HIF1α and HIF2α are dispensable for normal muscle development. At this stage, whether HIF3α plays a compensatory role in the absence of HIF1α and HIF2α has yet to be determined.

After muscle injury, skeletal muscle progenitor cells are challenged by hypoxia due to combined reduction of oxygen supply (caused by degeneration of blood vessels) and higher oxygen (or energy) demand during regeneration (36). Our data, consistent with previous studies show that HIF1α expression is elevated during muscle regeneration, whereas HIF2α is initially decreased but slowly increases during regeneration. These results indicate that HIFs may play stage-dependent roles during muscle regeneration. Our finding that satellite cell-specific HIF1α/HIF2α dKO mice exhibit delayed muscle regeneration is consistent with the reduced (but not completely absence of) satellite cells. Furthermore, our *in vitro* study demonstrates that hypoxia promotes satellite cell self-renewal in wild type myoblasts but not in HIF1α/HIF2α dKO myoblasts. These results indicate that hypoxia-enhanced self-renewal requires HIF1α and HIF2α.

Our previous research has demonstrated that hypoxia promotes satellite cell self-renewal and enhances the efficiency of myoblast transplantation (41). Additionally, the hypoxia-induced enhancement of self-renewal was highly dependent on activation of Notch signaling. Hypoxia also activates Notch signaling in other tissues (22, 47). In the present study we further show that hypoxia activates Notch signaling through HIF1α and HIF2α. Our conclusion is based on strong data showing that HIF1α/HIF2α dKO pharmacological inhibition of HIF1α/HIF2α abolishes hypoxia-elicited activation of Notch signaling and subsequent up-regulation of Pax7, the molecular determinant of self-renewal in satellite cells (12). In this regard the inability of hypoxia to activate Notch signaling underscores the self-renewal deficiencies of HIF1α/HIF2α dKO satellite cells.

In the present study we demonstrate that the HIF-Notch axis controls satellite cell self-renewal during adult muscle regeneration. We show for the first time that injury-induced increase of HIF1α and HIF2α contributes to the maintenance and long term homeostasis of satellite cells through promoting their self-renewal. Interestingly, we found that HIF1α and HIF2α are both dispensable for embryonic myogenesis. There are two potential explanations for this. First, even though developing embryos are in general exposed to a hypoxic environment, all cells in the embryo are not under the same hypoxic condition. It has been reported that cells in various regions of the embryo are challenged by different levels of hypoxia (48). Thus, embryonic muscle progenitors may be sufficiently oxygenated to render HIFs dispensable. As HIFs mediate hypoxia-induced activation

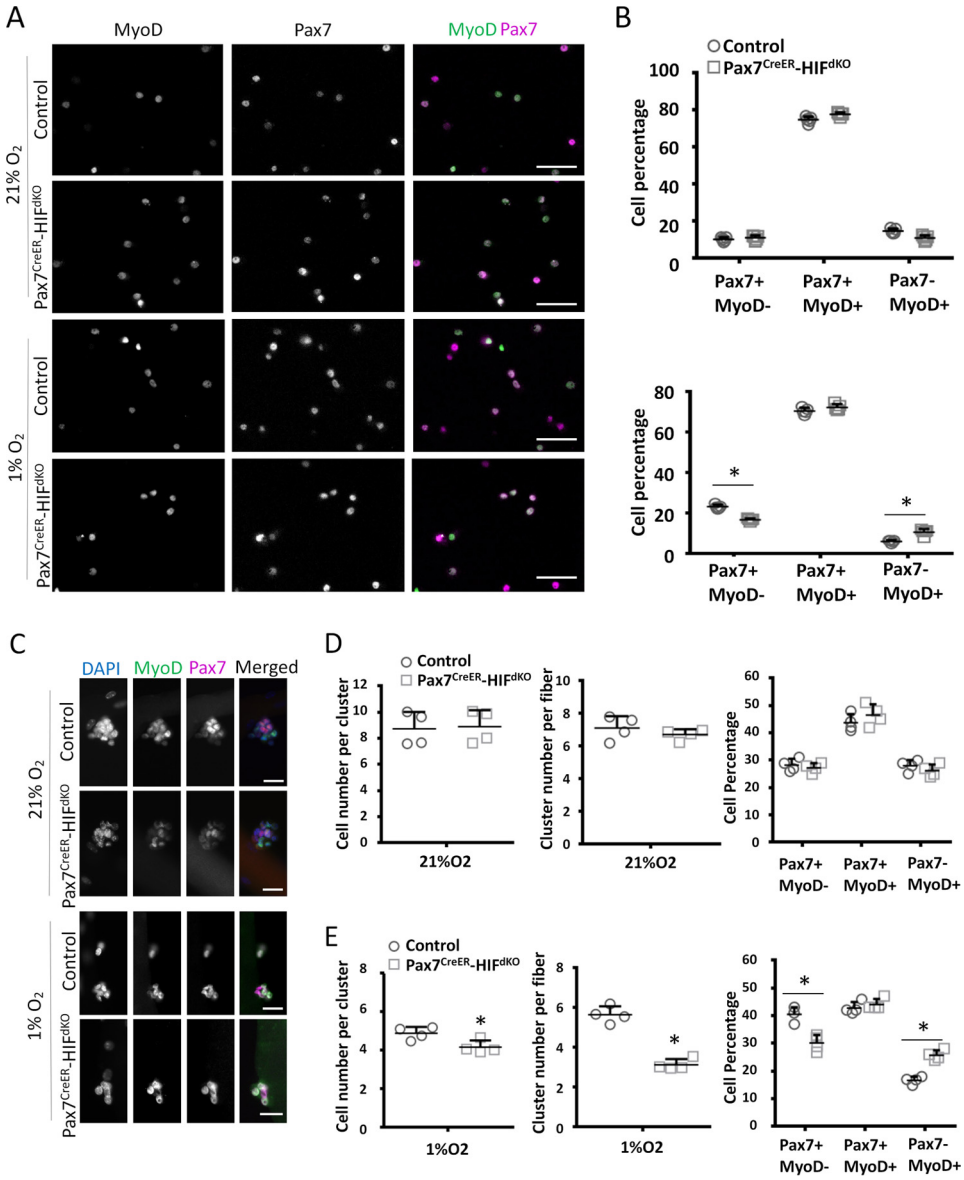

Figure 6. HIF1α/HIF2α deficiency inhibits self-renewal of satellite cells under hypoxia. *A*, representative images of $Pax7^{Cre}$-HIF^{dKO} and control primary myoblasts cultured under 21% O_2 (normoxia) or 1% O_2 (hypoxia) for 48 h and labeled with Pax7 (*purple*) and MyoD (*green*). *Scale bar*: 50 μm. *B*, percentage of self-renewed ($Pax7^+MyoD^-$), proliferating ($Pax7^+MyoD^+$), and differentiated ($Pax7^-MyoD^+$) cells. Cells collected from five pairs of control and HIF^{dKO} mice were used for analysis. For each batch of cells, 10 random areas were analyzed. *C*, represent images of freshly isolated myofibers after cultured under normoxia and hypoxia for 72 h and stained with Pax7 (*purple*) and MyoD (*green*). *Scale bar*: 25 μm. Single fibers were collected from 4 pairs of control and dKO mice, and 25 fibers were analyzed for each animal. *D*, number of myoblast clusters and cells/clusters. *E*, percentage of cells at different status at classified in *B*. Average values of each animal are shown. *Scale bar*: 50 μm. *Error bars* represent S.D. *, $p < 0.05$ (Student's *t* test, two-tailed).

of Notch signaling, an alternative possibility is that embryonic myoblasts exhibit sufficiently high levels of Notch signaling even in the absence of HIF1α and HIF2α. Supporting this notion, we show that activation of Notch signaling by Dll1 ligands rescues the self-renewal deficiencies of HIF1α/HIF2α dKO myoblasts. Indeed, it has been shown that muscle progenitors in embryonic stage intrinsically express high level of Notch (49). During injury, however, a temporal switch from Notch to Wnt signaling is required for normal adult myogenesis (50). Hence, hypoxia-induced activation of Notch may be necessary for switching a subpopulation of activated satellite cells to self-renewal, preventing excessive myogenic differentiation and maintaining a sustainable pool of satellite cells. The inability to activate Notch signaling in the HIF1α/HIF2α dKO satellite cells thus underlies the self-renewal defects. Our finding broadens the understanding of the mechanisms underlying satellite cell homeostasis during muscle regeneration. Such knowledge may lead to insights into development of novel therapies to treat muscle diseases or to improve muscle functions.

Experimental procedures

Animals

All animal experiments were approved by the Purdue Animal Care and Use Committee. Mice were housed in the animal facility with free access to water and standard rodent chow. All experimental mice were C57BL/6 from The Jackson Laboratory under catalogue no. 012476 ($Pax7^{CreER}$), no. 014140 ($MyoD^{Cre}$),

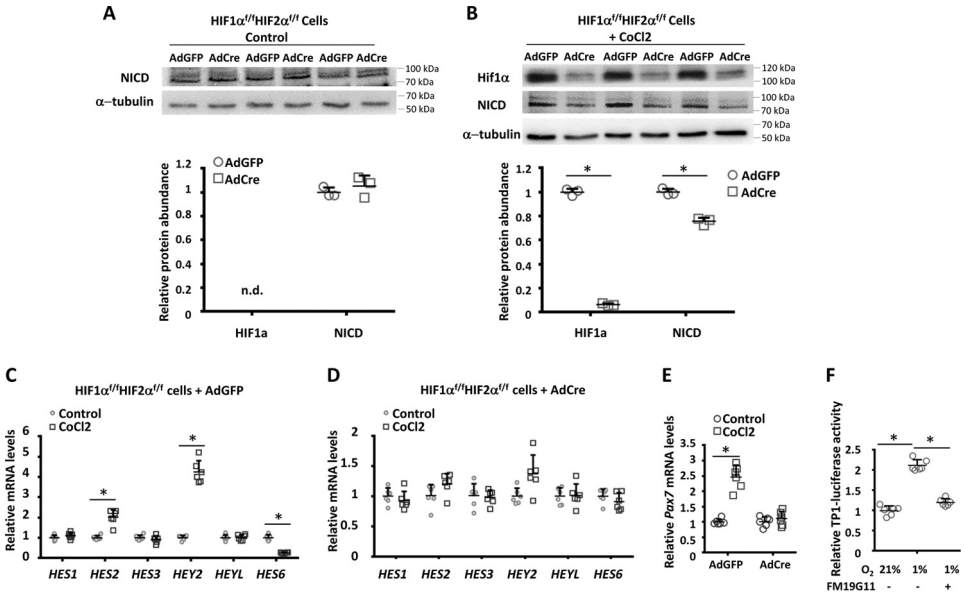

Figure 7. HIF1α and HIF2α are required for hypoxia-induced activation of Notch signaling and up-regulation of Pax7. Primary myoblasts from HIF1$\alpha^{f/f}$HIF2$\alpha^{f/f}$ mice were cultured in control medium or $CoCl_2$-containing medium (10 μM, to stabilize HIF1α/HIF2α and mimic hypoxia) and infected by adenovirus-GFP (*Ad-GFP*) or adenovirus (*Cre+GFP*), abbreviated as AdCre, at ~100 multiplicity of infection. *A*, relative protein levels of NICD in control myoblast; α-tubulin serves as the loading control. Please note that HIF1α bands are not shown because HIF1α is undetectable under normoxia. Relative protein abundance is quantified by densitometry using ImageJ after normalizing to α-tubulin levels and shown in the *lower bar graph*, $n = 3$ pairs. *B*, relative protein levels of NICD and HIF1α in HIF dKO myoblast; α-tubulin serves as the loading control. Relative protein abundance is quantified by densitometry using ImageJ after normalizing to α-tubulin levels and is shown in the *lower bar graph*. $n = 3$ pairs. *C* and *D*, relative mRNA levels of Notch target genes in AdGFP (*C*) and AdCre (*D*) transduced cells were measured by qPCR. *E*, relative mRNA levels of Pax7. *F*, relative Rpbj binding region luciferase activity in C2C12 cells under normoxia and hypoxia, with (+) or without (−) HIF1α/HIF2α inhibitor (FM19G11, 150 μM). For each group in *C–F*, six replicates were used for statistical analysis. *Error bars* represent S.D. *, $p < 0.05$ (Student's *t* test, two-tailed).

no. 007561 (HIF1$\alpha^{flox/flox}$), and no. 008407 (HIF2$\alpha^{flox/flox}$). PCR genotyping was done using protocols described by the supplier. Both male and female mice of 0–6 months old were used. Non-recombined animals were designated HIF1$\alpha^{f/f}$HIF2$\alpha^{f/f}$, and recombined animals were designated Pax7^{CreER}-HIF^{dKO} and MyoD-HIF^{dKO}, respectively.

Muscle injury and regeneration

CTX (50 μl, 10 μM, Sigma) was injected into the front of hind limb containing TA and EDL muscles to induce muscle regeneration. Regenerative TA and EDL muscles were harvested on the 7th and 21th day after CTX treatment.

Hematoxylin and eosin (H&E) staining

Muscles were frozen on dry ice in isopentane and 10-μm-thick cross-sections were cut with a Leica CM1850 cryostat (Leica, Wetzlar, Germany). Sections were stained in hematoxylin for 5 min followed by eosin staining for 2 min. Slides were then dehydrated with a sequential alcohol gradient (75, 95, and 100%) for 1 min each and cleared in xylene for 5 min and mounted with xylene-based mounting medium (Source Mount, catalogue no. 9277722). Images were captured with a Nikon D90 digital camera (Nikon, Tokyo, Japan) installed on a Nikon (Diaphot) inverted microscope after mounting.

Isolation and culture of single fibers

Intact EDL muscles from 10-week-old mice were digested in 0.2% collagenase I (Roche Applied Science) dissolved in Dulbecco's modified Eagle's medium (DMED, Sigma) for 30 min at 37 °C with gentle shaking every 5 min. Single fibers were dissociated by gently pipetting with glass pipettes. Isolated single fibers were fixed in 4% paraformaldehyde for immunostaining or cultured in horse serum-coated dishes in DMEM supplemented with 10% fetal bovine serum (FBS), 1% penicillin/streptomycin, and 0.1% fibroblast growth factor-basic for 3 days.

Isolation and culture of primary myoblasts

Mouse hind limb muscles were minced and digested in 2.5 ml of collagenase/dispase solution (10 μg/ml collagenase B, 2.4 units/ml dispase in PBS, Roche Applied Science) for 30 min. Digested cells were harvested and cultured in growth media (F-10 Ham's medium supplemented with 20% fetal bovine serum, 4 ng/ml fibroblast growth factor-basic, and 1% penicillin/streptomycin) on the collagen-coated dishes at 37 °C with 5% CO_2. Primary myoblasts were used for analysis after purification by 2–3 times of pre-plating. To induce the knockout of HIF1α and HIF2α in primary myoblasts, Pax7^{CreER}-HIF1$\alpha^{f/f}$HIF2$\alpha^{f/f}$ myoblasts were isolated and treated with 40 nM 4-OH-TMX (Sigma) for 2 days. Cells were then used for the analysis after removal of the 4-OH-TMX for 2 days. HIF1$\alpha^{f/f}$HIF2$\alpha^{f/f}$ cells were similarly treated as control. To activate Notch signaling in myoblasts, Dll1-overexpressing OP9 cells were first grown to 70% confluence in DMEM (45). Myoblasts were then seeded into the OP9 cells at an ~1:1 ratio and cultured for 3 days in Ham's F10 as described for culture of normal primary myoblasts.

Immunofluorescence

Muscle cryosections, single fibers, or cultured cells were fixed with 4% paraformaldehyde for 10 min and then were blocked in blocking buffer (5% goat serum, 2% BSA, 0.2% Triton

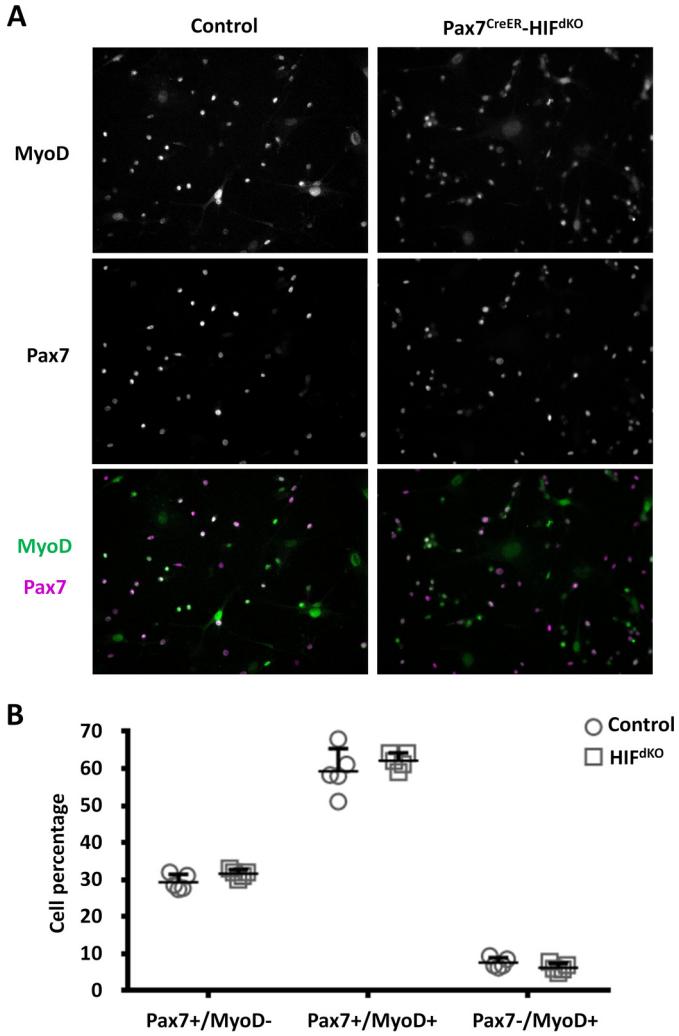

Figure 8. Activation of Notch signaling rescues self-renewal defects of HIF1α/HIF2α dKO myoblasts under hypoxia conditions. Primary myoblasts were co-cultured with Dll1-overexpressing OP9 cells to activate Notch signaling in control and HIF1α/HIF2α dKO myoblast. *A*, representative images of MyoD and Pax7 immunofluorescence in co-cultured control and HIF1α/HIF2α dKO (Pax7^{CreER}-HIF^{dKO} treated with 40 nM 4-OH-tamoxifen) myoblasts. *Scale bar*: 25 μm. *B*, percentages of Pax7^{+}/MyoD^{-}, Pax7^{+}/MyoD^{+}, and Pax7^{-}/MyoD^{+} cells quantified from images as shown in *A*. Cells collected from five pairs of control and HIF^{dKO} mice were used for analysis. For each batch of cells, 10 random areas were analyzed. Average values of each batch of cells are shown. *Error bars* represent S.D.

X-100, and 0.1% sodium azide in PBS) for 1 h at room temperature. Samples were incubated with primary antibody diluted in the same blocking buffer at 4 °C overnight followed by the incubation of 4′,6-diamidino-2-phenylindole (DAPI) and respective fluorescent-labeled secondary antibodies in room temperature for 1 h. The primary antibodies used as follows: Pax7 monoclonal antibody (mouse IgG1, Clone Pax7, Developmental Studies Hybridoma Bank, 1:20, cell culture supernatant); MyoD polyclonal antibody (rabbit IgG, M-318, Santa Cruz Biotechnology, 1:1000); Dystrophin polyclonal antibody (rabbit IgG, Ab15277, Abcam, 1:1000). All primary antibodies are commercially available and validated by the manufacturers. The second antibodies used were Alexa568 goat anti-mouse IgG1 and Alexa486 goat anti-rabbit IgG (Invitrogen). Images were captured with Coolsnap HQ CCD camera (Photometrics) driven by IP Lab software (Scanalytics Inc) using Leica DMI 6000B fluorescent microscope (Mannheim, Germany). Quantification of myofiber size was conducted by Image J software (freely available from National Institutes of Health). Self-renewal assay was conducted as previously described (41). Briefly, the relative intensity of Pax7 and MyoD immunofluorescence was used to classify the cell cycle state of myoblasts. If the merged photos show Pax7 single positive then cells were classified as self-renewal, MyoD single positive cells were classified as differentiation, and double positive cells were considered as proliferation.

Induction of hypoxia

Hypoxia was induced as previously described (41, 51). Briefly, cells were cultured in a gas-tight modular incubator chamber flushed with a custom gas mixture containing 5% air, 5% CO_2, and 90% N2, 30 p.s.i./min for 2.5 min each day to achieve 1% O_2 hypoxic environment in the chamber. Alternatively, $CoCl_2$ (10 μM) were used to stabilize HIF1α and mimic hypoxia stimulation. In this case cells were treated with $CoCl_2$ for 6 h.

Gene expression analysis

Total RNA was extracted by TRIzol (Sigma) according to the manufacturer's instructions. 4 μg of RNA was converted into cDNA by random hexamer primers with Moloney murine leukemia virus reverse transcriptase. Quantitative real-time polymerase chain reaction (qPCR) analysis was performed with a SYBR Green PCR kit in a Roche Lightcycler 480 system (Roche Applied Science). All primers used are listed in supplemental Table 1. Gene expression was calculated with the $2^{-\Delta\Delta CT}$ relative quantification method and normalized to 18S.

Western blot

Total protein from cells and tissues was extracted with radioimmune precipitation assay buffer (pH 8.0, 50 mM Tris-HCL, 150 mM NaCl, 1%Nonidet P-40, 0.5% sodium deoxycholate and 0.1% SDS). Protein concentration was determined by BCA Protein Assay Reagent (Pierce). Equal amounts of proteins were separated by SDS-PAGE and transferred to a polyvinylidene difluoride membrane (Millipore Corp., Billerica, MA). Membranes were then blocked in 5% milk and incubated with diluted primary antibodies overnight at 4 °C followed by secondary antibodies for 1 h at room temperature. Primary antibodies (all rabbit polyclonal) used were HIF1α (NB100–105, Novus Biologicals; 1:500), NICD (ab8925, Abcam; 1:2000), α-tubulin (B-7, Santa Cruz, CA; 1:1000), and GAPDH (sc-32233, Santa Cruz Biotechnology, 1:2000). All primary antibodies are commercially available and validated by the manufacturers. Secondary antibodies (anti-rabbit IgG or anti-mouse IgG; Jackson ImmunoResearch) were diluted 2000-fold. Signals were detected by using enhanced chemiluminescence Western blotting substrate (Pierce) or fluorescence on a FluorChem R protein imaging system (Protein Simple, CA).

Luciferase assay

C2C12 cell lines were transfected with Renilla and Rpbj binding domain luciferase reporter (TP-1). Cells were then treated in three parallel groups. Group I cells were maintained under normoxia for 48 h without FM19G11 (Santa Cruz Biotechnology, catalog #sc-364490), a pharmacological inhibitor of HIF1a/

HIF2a. Group II cells were cultured at 1% O_2 for 48 h without FM19G11. Group III cells were cultured at 1% O_2 and treated with 150 μM FM19G11.

Statistical analysis

Data are presented as the mean and S.D. Numbers of repeats represent biological repeats (number of mice or batches of primary cells) unless otherwise indicated. Samples were randomized during data collection. Investigators are not blinded to the group allocation during data acquisition. All analyses were conducted with Student's *t* test with a two-tail distribution; comparisons with values of $p < 0.05$ were considered statistically significant.

Author contributions—X. Y. and S. Y. performed the experiments, analyzed the data, prepared the figures, and drafted the manuscript. C. W. prepared the figures and revised the manuscript. S. K. designed the study, analyzed the data, and drafted and revised the manuscript. All authors reviewed the results and approved the final version of the manuscript.

Acknowledgments—We thank Nadia Carlesso (Indiana University School of Medicine) for providing the Dll1 overexpression OP9 cells and Yaohui Nie and Hannah Horton for careful reading of the manuscript. We thank Jun Wu for laboratory management and maintaining mouse colonies and other members of the Kuang laboratory for technical assistance and discussions.

References

1. Sambasivan, R., Yao, R., Kissenpfennig, A., Van Wittenberghe, L., Paldi, A., Gayraud-Morel, B., Guenou, H., Malissen, B., Tajbakhsh, S., and Galy, A. (2011) Pax7-expressing satellite cells are indispensable for adult skeletal muscle regeneration. *Development* **138,** 3647–3656
2. Lepper, C., Partridge, T. A., and Fan, C. M. (2011) An absolute requirement for Pax7-positive satellite cells in acute injury-induced skeletal muscle regeneration. *Development* **138,** 3639–3646
3. Montarras, D., Morgan, J., Collins, C., Relaix, F., Zaffran, S., Cumano, A., Partridge, T., and Buckingham, M. (2005) Direct isolation of satellite cells for skeletal muscle regeneration. *Science* **309,** 2064–2067
4. Relaix, F., and Zammit, P. S. (2012) Satellite cells are essential for skeletal muscle regeneration: the cell on the edge returns centre stage. *Development* **139,** 2845–2856
5. Rocheteau, P., Gayraud-Morel, B., Siegl-Cachedenier, I., Blasco, M. A., and Tajbakhsh, S. (2012) A subpopulation of adult skeletal muscle stem cells retains all template DNA strands after cell division. *Cell* **148,** 112–125
6. Brack, A. S., and Rando, T. A. (2012) Tissue-specific stem cells: lessons from the skeletal muscle satellite cell. *Cell Stem Cell* **10,** 504–514
7. Collins, C. A., Olsen, I., Zammit, P. S., Heslop, L., Petrie, A., Partridge, T. A., and Morgan, J. E. (2005) Stem cell function, self-renewal, and behavioral heterogeneity of cells from the adult muscle satellite cell niche. *Cell* **122,** 289–301
8. Halevy, O., Piestun, Y., Allouh, M. Z., Rosser, B. W., Rinkevich, Y., Reshef, R., Rozenboim, I., Wleklinski-Lee, M., and Yablonka-Reuveni, Z. (2004) Pattern of Pax7 expression during myogenesis in the posthatch chicken establishes a model for satellite cell differentiation and renewal. *Dev. Dyn* **231,** 489–502
9. Olguin, H. C., and Olwin, B. B. (2004) Pax-7 up-regulation inhibits myogenesis and cell cycle progression in satellite cells: a potential mechanism for self-renewal. *Dev. Biol.* **275,** 375–388
10. Zammit, P. S., Golding, J. P., Nagata, Y., Hudon, V., Partridge, T. A., and Beauchamp, J. R. (2004) Muscle satellite cells adopt divergent fates: a mechanism for self-renewal? *J. Cell Biol.* **166,** 347–357
11. Bjornson, C. R., Cheung, T. H., Liu, L., Tripathi, P. V., Steeper, K. M., and Rando, T. A. (2012) Notch signaling is necessary to maintain quiescence in adult muscle stem cells. *Stem Cells* **30,** 232–242
12. Wen, Y., Bi, P., Liu, W., Asakura, A., Keller, C., and Kuang, S. (2012) Constitutive notch activation upregulates Pax7 and promotes the self-renewal of skeletal muscle satellite cells. *Mol. Cell. Biol.* **32,** 2300–2311
13. Kuang, S., Gillespie, M. A., and Rudnicki, M. A. (2008) Niche regulation of muscle satellite cell self-renewal and differentiation. *Cell Stem Cell* **2,** 22–31
14. Yin, H., Price, F., and Rudnicki, M. A. (2013) Satellite cells and the muscle stem cell niche. *Physiol. Rev.* **93,** 23–67
15. Provot, S., Zinyk, D., Gunes, Y., Kathri, R., Le, Q., Kronenberg, H. M., Johnson, R. S., Longaker, M. T., Giaccia, A. J., and Schipani, E. (2007) Hif-1α regulates differentiation of the limb bud mesenchyme and joint development. *J. Cell Biol.* **177,** 451–464
16. Simon, M. C., and Keith, B. (2008) The role of oxygen availability in embryonic development and stem cell function. *Nat. Rev. Mol. Cell Biol.* **9,** 285–296
17. Huang, L. E., Arany, Z., Livingston, D. M., and Bunn, H. F. (1996) Activation of hypoxia-inducible transcription factor depends primarily upon redox-sensitive stabilization of its α subunit. *J. Biol. Chem.* **271,** 32253–32259
18. Drevytska, T., Gavenauskas, B., Drozdovska, S., Nosar, V., Dosenko, V., and Mankovska, I. (2012) HIF-3α mRNA expression changes in different tissues and their role in adaptation to intermittent hypoxia and physical exercise. *Pathophysiology* **19,** 205–214
19. Zagórska, A., and Dulak, J. (2004) HIF-1: the knowns and unknowns of hypoxia sensing. *Acta Biochim. Pol.* **51,** 563–585
20. Kubis, H. P., Hanke, N., Scheibe, R. J., and Gros, G. (2005) Accumulation and nuclear import of HIF1 α during high and low oxygen concentration in skeletal muscle cells in primary culture. *Biochim. Biophys. Acta* **1745,** 187–195
21. Krinner, A., Zscharnack, M., Bader, A., Drasdo, D., and Galle, J. (2009) Impact of oxygen environment on mesenchymal stem cell expansion and chondrogenic differentiation. *Cell Prolif.* **42,** 471–484
22. Eliasson, P., and Jönsson, J. I. (2010) The hematopoietic stem cell niche: low in oxygen but a nice place to be. *J. Cell. Physiol.* **222,** 17–22
23. Sakagami, H., Makino, Y., Mizumoto, K., Isoe, T., Takeda, Y., Watanabe, J., Fujita, Y., Takiyama, Y., Abiko, A., and Haneda, M. (2014) Loss of HIF-1α impairs GLUT4 translocation and glucose uptake by the skeletal muscle cells. *Am. J. Physiol. Endocrinol. Metab.* **306,** E1065–E1076
24. Mason, S. D., Howlett, R. A., Kim, M. J., Olfert, I. M., Hogan, M. C., McNulty, W., Hickey, R. P., Wagner, P. D., Kahn, C. R., Giordano, F. J., and Johnson, R. S. (2004) Loss of skeletal muscle HIF-1α results in altered exercise endurance. *Plos Biol.* **2,** e288
25. Rasbach, K. A., Gupta, R. K., Ruas, J. L., Wu, J., Naseri, E., Estall, J. L., and Spiegelman, B. M. (2010) PGC-1α regulates a HIF2α-dependent switch in skeletal muscle fiber types. *Proc. Natl. Acad. Sci. U.S.A.* **107,** 21866–21871
26. Lunde, I. G., Anton, S. L., Bruusgaard, J. C., Rana, Z. A., Ellefsen, S., and Gundersen, K. (2011) Hypoxia inducible factor 1 links fast-patterned muscle activity and fast muscle phenotype in rats. *J. Physiol.* **589,** 1443–1454
27. Loboda, A., Jozkowicz, A., and Dulak, J. (2012) HIF-1 *versus* HIF-2: Is one more important than the other? *Vascul. Pharmacol.* **56,** 245–251
28. Li, Q. F., and Dai, A. G. (2005) Differential expression of three hypoxia-inducible factor-α subunits in pulmonary arteries of rat with hypoxia-induced hypertension. *Acta Biochim. Biophys. Sin.* **37,** 665–672
29. Ono, Y., Sensui, H., Sakamoto, Y., and Nagatomi, R. (2006) Knockdown of hypoxia-inducible factor-1α by siRNA inhibits C2C12 myoblast differentiation. *J. Cell. Biochem.* **98,** 642–649
30. Majmundar, A. J., Lee, D. S., Skuli, N., Mesquita, R. C., Kim, M. N., Yodh, A. G., Nguyen-McCarty, M., Li, B., and Simon, M. C. (2015) HIF modulation of Wnt signaling regulates skeletal myogenesis *in vivo*. *Development* **142,** 2405–2412
31. Gustafsson, M. V., Zheng, X., Pereira, T., Gradin, K., Jin, S., Lundkvist, J., Ruas, J. L., Poellinger, L., Lendahl, U., and Bondesson, M. (2005) Hypoxia requires notch signaling to maintain the undifferentiated cell state. *Dev. Cell* **9,** 617–628

32. Villa, J. C., Chiu, D., Brandes, A. H., Escorcia, F. E., Villa, C. H., Maguire, W. F., Hu, C. J., de Stanchina, E., Simon, M. C., Sisodia, S. S., Scheinberg, D. A., and Li, Y. M. (2014) Nontranscriptional role of Hif-1 α in activation of γ-secretase and notch signaling in breast cancer. *Cell Rep.* **8,** 1077–1092
33. Forristal, C. E., Wright, K. L., Hanley, N. A., Oreffo, R. O., and Houghton, F. D. (2010) Hypoxia inducible factors regulate pluripotency and proliferation in human embryonic stem cells cultured at reduced oxygen tensions. *Reproduction* **139,** 85–97
34. Iyer, N. V., Kotch, L. E., Agani, F., Leung, S. W., Laughner, E., Wenger, R. H., Gassmann, M., Gearhart, J. D., Lawler, A. M., Yu, A. Y., and Semenza, G. L. (1998) Cellular and developmental control of O2 homeostasis by hypoxia-inducible factor 1 α. *Genes Dev.* **12,** 149–162
35. Compernolle, V., Brusselmans, K., Acker, T., Hoet, P., Tjwa, M., Beck, H., Plaisance, S., Dor, Y., Keshet, E., Lupu, F., Nemery, B., Dewerchin, M., Van Veldhoven, P., Plate, K., Moons, L., Collen, D., and Carmeliet, P. (2002) Loss of HIF-2α and inhibition of VEGF impair fetal lung maturation, whereas treatment with VEGF prevents fatal respiratory distress in premature mice. *Nat. Med.* **8,** 702–710
36. Merrick, M. A. (2002) Secondary injury after musculoskeletal trauma: a review and update. *J. Athl Train.* **37,** 209–217
37. Kuang, S., and Rudnicki, M. A. (2008) The emerging biology of satellite cells and their therapeutic potential. *Trends Mol. Med.* **14,** 82–91
38. Seale, P., Sabourin, L. A., Girgis-Gabardo, A., Mansouri, A., Gruss, P., and Rudnicki, M. A. (2000) Pax7 is required for the specification of myogenic satellite cells. *Cell* **102,** 777–786
39. Beauchamp, J. R., Heslop, L., Yu, D. S., Tajbakhsh, S., Kelly, R. G., Wernig, A., Buckingham, M. E., Partridge, T. A., and Zammit, P. S. (2000) Expression of CD34 and Myf5 defines the majority of quiescent adult skeletal muscle satellite cells. *J. Cell Biol.* **151,** 1221–1234
40. Wang, Y. X., Dumont, N. A., and Rudnicki, M. A. (2014) Muscle stem cells at a glance. *J. Cell Sci.* **127,** 4543–4548
41. Liu, W., Wen, Y., Bi, P., Lai, X., Liu, X. S., Liu, X., and Kuang, S. (2012) Hypoxia promotes satellite cell self-renewal and enhances the efficiency of myoblast transplantation. *Development* **139,** 2857–2865
42. Katz, B., and Miledi, R. (1961) The localized action of end-plate drugs' in the twitch fibres of the frog. *J. Physiol.* **155,** 399–415
43. Kopan, R., Nye, J. S., and Weintraub, H. (1994) The intracellular domain of mouse notch: a constitutively activated repressor of myogenesis directed at the basic helix-loop-helix region of Myod. *Development* **120,** 2385–2396
44. Conboy, I. M., and Rando, T. A. (2002) The regulation of notch signaling controls satellite cell activation and cell fate determination in postnatal myogenesis. *Dev. Cell* **3,** 397–409
45. Schmitt, T. M., and Zúñiga-Pflücker, J. C. (2002) Induction of T cell development from hematopoietic progenitor cells by delta-like-1 *in vitro*. *Immunity* **17,** 749–756
46. Kim, H., Huang, L., Critser, P. J., Yang, Z., Chan, R. J., Wang, L., Carlesso, N., Voytik-Harbin, S. L., Bernstein, I. D., and Yoder, M. C. (2015) Notch ligand Delta-like 1 promotes *in vivo* vasculogenesis in human cord blood-derived endothelial colony forming cells. *Cytotherapy* **17,** 579–592
47. Clarke, L., and van der Kooy, D. (2009) Low oxygen enhances primitive and definitive neural stem cell colony formation by inhibiting distinct cell death pathways. *Stem Cells* **27,** 1879–1886
48. Ream, M., Ray, A. M., Chandra, R., and Chikaraishi, D. M. (2008) Early fetal hypoxia leads to growth restriction and myocardial thinning. *Am. J. Physiol. Regul. Integr. Comp. Physiol.* **295,** R583–R595
49. Vasyutina, E., Lenhard, D. C., Wende, H., Erdmann, B., Epstein, J. A., and Birchmeier, C. (2007) RBP-J (Rbpsuh) is essential to maintain muscle progenitor cells and to generate satellite cells. *Proc. Natl. Acad. Sci. U.S.A.* **104,** 4443–4448
50. Brack, A. S., Conboy, I. M., Conboy, M. J., Shen, J., and Rando, T. A. (2008) A temporal switch from Notch to Wnt signaling in muscle stem cells is necessary for normal adult myogenesis. *Cell Stem Cell* **2,** 50–59
51. Wang, C., Liu, W., Liu, Z., Chen, L., Liu, X., and Kuang, S. (2015) Hypoxia inhibits myogenic differentiation through p53 protein-dependent induction of bhlhe40 protein. *J. Biol. Chem.* **290,** 29707–29716

The hypoxia-inducible factors HIF1α and HIF2α are dispensable for embryonic muscle development but essential for postnatal muscle regeneration

Xin Yang, Shiqi Yang, Chao Wang and Shihuan Kuang

J. Biol. Chem. 2017, 292:5981-5991.
doi: 10.1074/jbc.M116.756312 originally published online February 23, 2017